



# MINT: Multi-modal Chain of Thought in Unified Generative Models for Enhanced Image Generation

Yi Wang<sup>1,2\*</sup> Mushui Liu<sup>1,2\*</sup> Wanggui He<sup>2,\*†</sup> Longxiang Zhang<sup>2,+†</sup> Ziwei Huang<sup>1,2,+†</sup> Guanghao Zhang<sup>2,+†</sup>  
Fangxun Shu<sup>2</sup> ZhongTao<sup>2</sup> Dong She<sup>2</sup> Zhelun Yu<sup>2</sup> Haoyuan Li<sup>2</sup> Weilong Dai<sup>2</sup> Mingli Song<sup>1</sup>  
Jie Song<sup>1,‡</sup> Hao Jiang<sup>2,‡</sup>

<sup>1</sup>Zhejiang University <sup>2</sup>Alibaba Group

\*Equal contribution †Project lead +Core contributor ‡Corresponding author

{y-w, lms, 22351096, sjie, brooksong}@zju.edu.cn

{wanggui.hwg, shengxiang.zlx, guanghai.zgh, junmu.dwl, aoshu.jh}@taobao.com

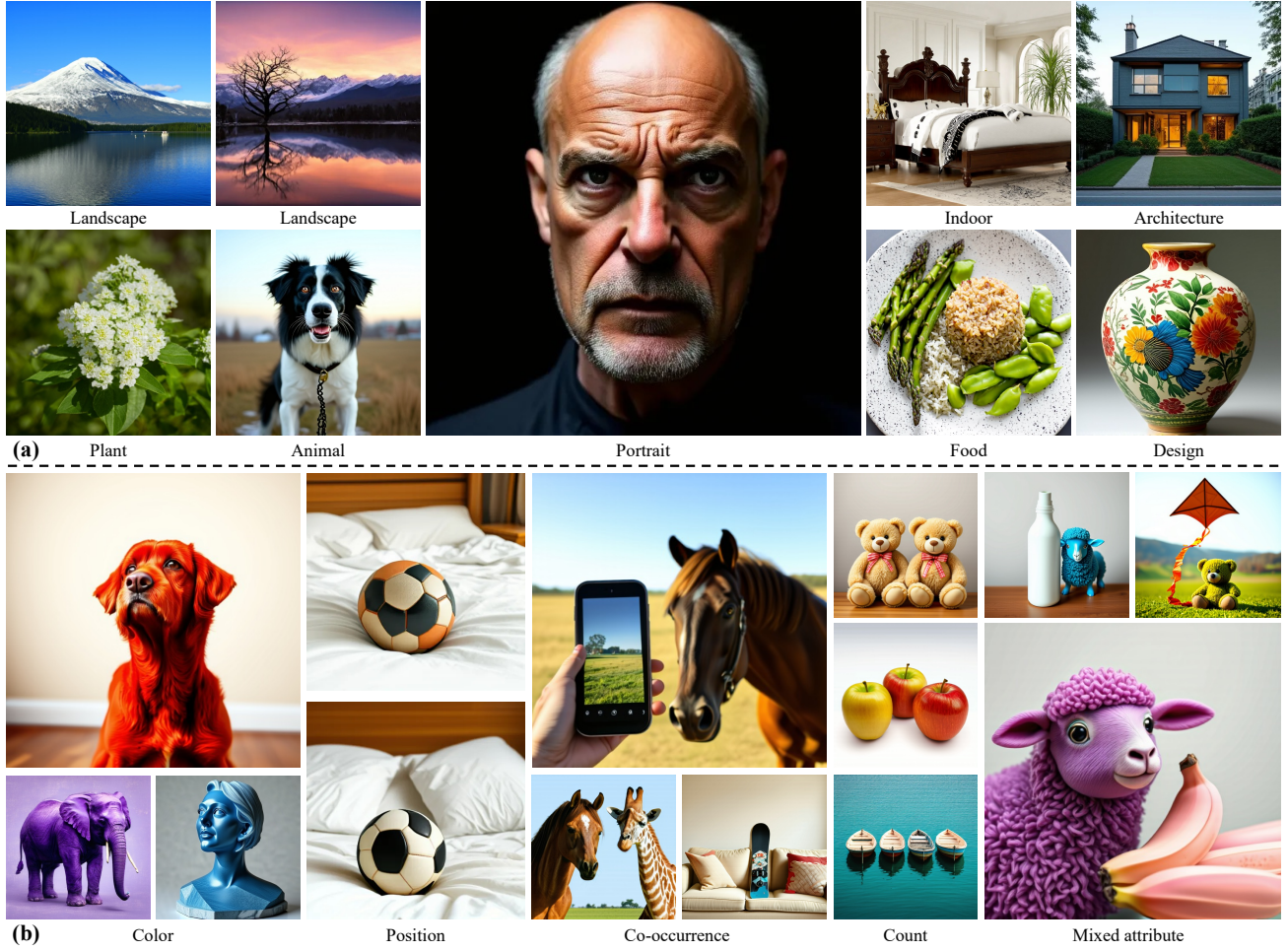


Figure 1: Visualization of images generated by MINT. (a) Images with various themes generated by MINT demonstrate its exceptional versatility while exhibiting extraordinary detail quality. (b) Integrated with Multimodal Chain of Thought (MCoT), MINT exhibits remarkable capabilities in understanding and reasoning about text-image relationships, effectively adhering to the interwoven conditions present in intricate imagery.

## Abstract

Unified generative models have demonstrated extraordinary performance in both text and image generation. However, they tend to underperform when generating intricate images with various interwoven conditions, which is hard to solely rely on straightforward text-to-image generation. In response to this challenge, we introduce **MINT**, an innovative unified generative model, empowered with native multimodal chain of thought (MCoT) for enhanced image generation for the first time. Firstly, we design Mixture of Transformer Experts (MTXpert), an expert-parallel structure that effectively supports both natural language generation (NLG) and visual capabilities, while avoiding potential modality conflicts that could hinder the full potential of each modality. Building on this, we propose an innovative MCoT training paradigm—a step-by-step approach to multimodal thinking, reasoning, and reflection specifically designed to enhance image generation. This paradigm equips MINT with nuanced, element-wise decoupled alignment and a comprehensive understanding of textual and visual components. Furthermore, it fosters advanced multimodal reasoning and self-reflection, enabling the construction of images that are firmly grounded in the logical relationships between these elements. Notably, MINT has been validated to exhibit superior performance across multiple benchmarks for text-to-image (T2I) and image-to-text (I2T) tasks.

## 1. Introduction

Unified generative models (Kondratyuk et al., 2023; He et al., 2024; Bachmann et al., 2024; Zhou et al., 2024b) have recently demonstrated superior capabilities in understanding and generating multimodal information, e.g., linguistic and visual data. Prior works (Ding et al., 2021; Team, 2024b; Lu et al., 2024; Kondratyuk et al., 2023) employ next-token prediction frameworks that represent all modalities as discrete tokens to capture cross-modal interactions. However, such discrete tokenization approaches do not align with the continuous nature of images and videos, thereby limiting the generative potential.

To address these limitations, recent studies (Zhou et al., 2024b; Xiao et al., 2024; Ma et al., 2024) have explored hybrid generative models that process images as continuous data using diffusion manner and text as discrete data through an autoregressive manner. These models can achieve comparable and even superior performance to diffusion models in image generation tasks. However, as illustrated in Figure 2, when generating intricate images—particularly



Figure 2: Limitations of straightforward text-to-image (T2I) generation. (a) T2I generation results illustrate confusion and defects. (b) The results generated by MINT with MCoT effectively address these issues.

those with various interwoven conditions, a straightforward text-to-image (T2I) approach often falls short of meeting users’ expectations in a single attempt. This necessitates models with exceptionally strong fine-grained image-text alignment, concept-wise understanding, and reasoning capabilities, which is precisely what we anticipate unified generative models will ultimately achieve, due to their inherent advantage of multimodal information interaction within a single model. Therefore, a natural question arises: *Is it feasible to harness the multimodal understanding, reasoning, and generative capabilities of unified generative models to effectively address such intricate and realistic multimodal challenges in a step-by-step manner?*

In this paper, we introduce **MINT**, an innovative unified generative model, empowered by **multimodal chain of thought (MCoT)** for enhanced image generation. MCoT represents step-by-step multimodal thinking and reasoning, akin to the chain of thought (CoT) (Wei et al., 2022b), thereby further unlocking the multimodal potential of unified generative models. To achieve this, as shown in Figure 3, we firstly design the **Mixture of Transformer Experts (MTXpert)** as the core of MINT, which preserves the natural language processing capabilities of pretrained large language models while seamlessly endowing the model with exceptional visual understanding and generative abilities. Moreover, MTXpert, an expert-parallel design, avoids potential conflicts between different modalities that can occur in a single Transformer model (Liang et al., 2024a; Shi et al., 2024), thereby facilitating a comprehensive interplay and deep alignment between the textual and visual modalities, which is vital for unlocking multimodal thinking and reasoning.

Finally, and most importantly, to activate the inherent MCoT skill set of MINT, we propose an innovative MCOT training paradigm, as illustrated in Figure 3. Generating intricate images—such as those featuring multiple objects, complex spatial relationships, and various attributes that are all interwoven—requires nuanced, element-wise decou-

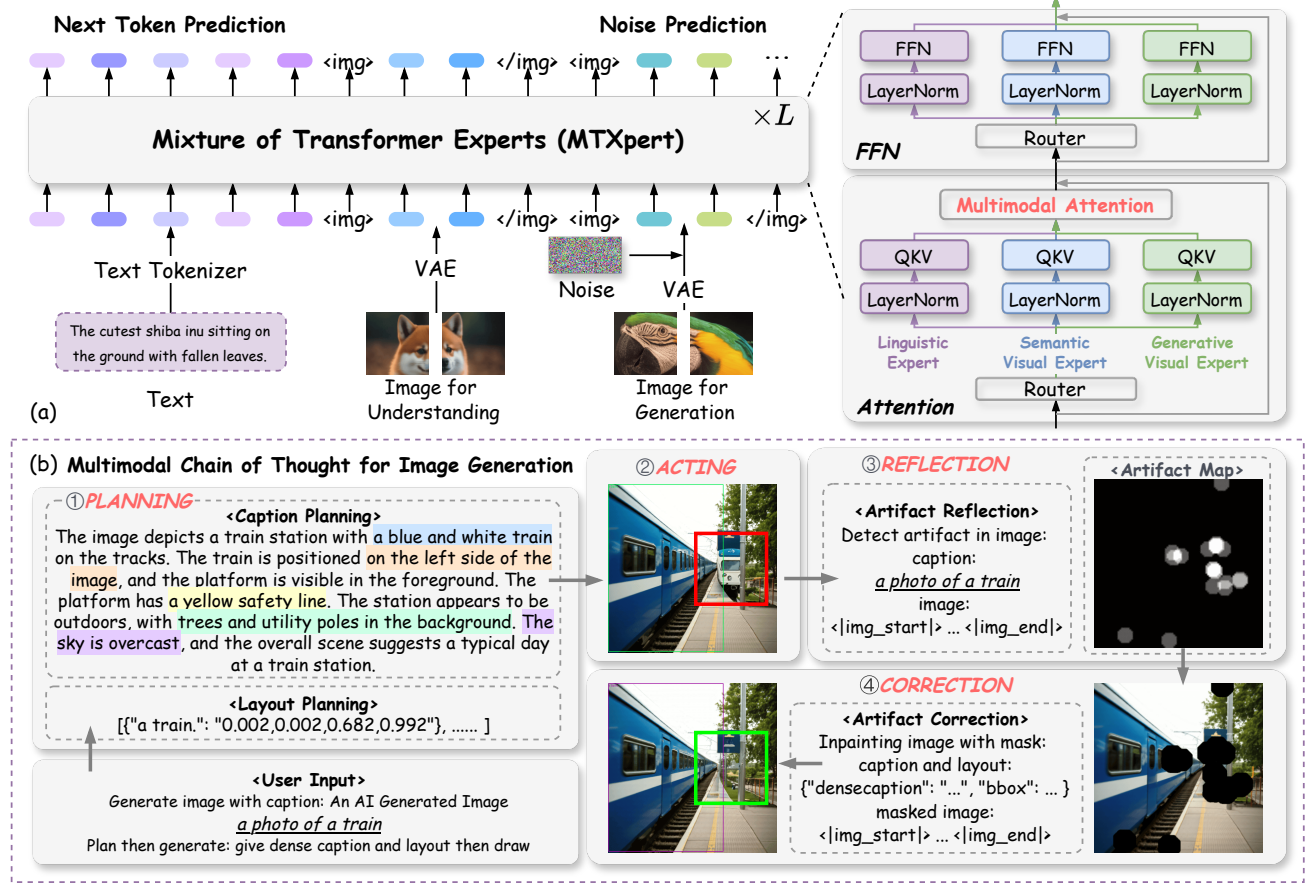


Figure 3: Overall Framework of the Proposed MINT. (a) The illustration of MINT architecture, highlighting expert-parallel MTXpert as the core component. (b) Multimodal Chain of Thought (MCoT) empowers MINT with nuanced, element-wise decoupled alignment, facilitating advanced multimodal thinking and reasoning capabilities.

pled alignment and a deep understanding of textual and visual components. This process further entails the ability to fully comprehend the semantic connections among these elements and their corresponding text, thereby enabling the construction of images that are firmly grounded in the logical relationships between them. However, straightforward T2I generation is insufficient to effectively address these challenges. To overcome these limitations, we introduce the MCoT training paradigm to equip MINT with native MCoT capabilities. MCoT replaces the straightforward T2I process with step-by-step multimodal thinking, reasoning, and reflection, thereby alleviating the difficulties associated with generating intricate images. All MCoT steps are handled entirely within MINT as shown in Figure 3, where the planning and acting steps explicitly enhance fine-grained alignment between text and images, as well as the decoupling of visual elements. Furthermore, the reflection and correction steps enable the model to self-assess artifacts within the generated image and identify discrepancies between the image and the corresponding caption, which endows MINT with human-like evaluative capabilities, further refining image details

and ultimately improving the quality of image generation.

In general, our contributions can be summarized as follows:

- We introduce MINT, a unified generative model that seamlessly integrates understanding and generation capabilities of both textual and visual data. MINT decouples the model parameters associated with different tasks, specifically text generation, image understanding, and image generation, including feed-forward networks, attention matrices, and layer normalization. Further, it facilitates task-specific processing using global self-attention over the entire input sequence, resulting in superior performance in multimodal tasks and demonstrating the potential for expansion to any-to-any tasks.
- We propose the MCoT training paradigm to activate the native MCoT capabilities of unified generative models for the first time, thereby revealing previously untapped potential within large-scale text-image pre-training and demonstrating its effectiveness in enhancing perfor-

mance for intricate and realistic multimodal challenges, such as intricate image generation.

- MINT demonstrates an enhanced ability in multimodal thinking and reasoning, enabling it to effectively break down complex problems and achieve exceptional performance, which is validated across a series of multimodal benchmarks, including GenEval, MS-COCO, VQA-v2, MME, and MMBench.

## 2. Related Works

**Generative Foundation Models.** The GPT series (OpenAI, 2023) have demonstrated that language models can learn numerous tasks via training on a large-scale dataset. Beyond language, multi-modal large language models (Liu et al., 2023; Chen et al., 2024) have been proposed to integrate vision and language capabilities. However, they lack the capability to generate images. Some works propose integrating large language models (LLMs) with diffusion models to equip LLMs with image generation capability (Sun et al., 2024a; Ge et al., 2024b; Wu et al., 2024b). Others use discrete tokens to support both image and text generation simultaneously (Team, 2024a; Lu et al., 2024; Xie et al., 2024b). They focus on multi-modal generation with limited image-generation capability. Concurrent works such as TransFusion (Zhou et al., 2024a) and Show-O (Xie et al., 2024b) unify diffusion and autoregressive methods into a single model, generating text autoregressively and images through diffusion. Nonetheless, like existing diffusion models, these works focus on a limited range of image generation tasks, primarily text-to-image generation, and cannot cover more complex and various visual generation tasks.

**Diffusion Model.** Recent advancements in diffusion models have been remarkable, with notable contributions from the Stable Diffusion (SD) series (Rombach et al., 2022; Podell et al., 2024; Esser et al., 2024a), DALL-E (Ramesh et al., 2022), and Imagen (Ho et al., 2022). These models are predominantly designed for text-to-image generation tasks. Many efforts have been made to extend the capabilities of diffusion models, including ControlNet (Zhang et al., 2023), T2I-Adapter (Mou et al., 2024), and StyleShot (Gao et al., 2024). InstructPix2Pix (Brooks et al., 2023), and EMU-edit (Sheynin et al., 2024) explore performing general image editing tasks through instructions. However, these methods are task-specific, extending the capabilities of SD by modifying the model architecture. Some work explores the unification of computer vision tasks (Gan et al., 2023; Geng et al., 2024). However, these efforts primarily focus on traditional vision tasks instead of general image generation tasks and often underperform compared to models specifically designed and trained for corresponding tasks.

**Chain of Thought (CoT).** CoT aims to improve the model’s complex reasoning capabilities by correcting it step by step, which has been widely explored in language models (Wei et al., 2022a; Geva et al., 2021), yet still remains unexplored in image generation. Recent MLLMs such as LLaVA-CoT (Xu et al., 2024) leverage the LLMs to understand the visual content. In this work, we introduce Multimodal Chain of Thought to reveal the multimodal potential of a unified generative model, particularly for enhancing image generation.

## 3. Method

In this section, we will introduce the specific methodological details of the MINT model. In Section 3.1, we present the preliminaries, explaining the fundamental principles of text generation and image generation, and introducing the basic symbolic definitions. Section 3.2 elaborates on the architectural design of the MINT model, explaining the principles and functions of each module. Section 3.3 details the steps of the MCoT for image generation. In Appendix A and B, we present the detail of training strategy and the methodology for constructing the data required for training.

### 3.1. Preliminaries

**Language Modeling.** Let  $z = (z_1, \dots, z_N) \in V^N$  denote discrete token sequences with vocabulary  $V$ . Autoregressive language models implement the joint distribution through causal factorization:

$$P(z) = \prod_{i=1}^N P_\theta(z_i | z_{<i}) \quad (1)$$

where  $\theta$  parameterizes the conditional distributions. Training minimizes the language modeling objective:

$$\mathcal{L}_{\text{LM}} = \mathbb{E}_{z \sim \mathcal{D}} \left[ - \sum_{i=1}^N \log P_\theta(z_i | z_{<i}) \right] \quad (2)$$

For multimodal data pairs  $(x, c)$  with images  $x$  and captions  $c$ , we extend the condition to  $P_\theta(z_i | z_{<i}, \phi(x))$ , where  $\phi(\cdot)$  encodes visual features.

**Rectified Flow.** Given image data  $\mathbf{x} \sim \mathcal{D}$  and noise  $\epsilon \sim \mathcal{N}(0, I)$ , we construct linear trajectories:

$$\mathbf{x}_t = t\mathbf{x} + (1-t)\epsilon, \quad t \in [0, 1] \quad (3)$$

The velocity field model  $v_\theta$  predicts straightening directions through:

$$\mathcal{L}_{\text{RF}} = \mathbb{E}_{t \sim U(0,1), \mathbf{x}, \epsilon, c} [\|(\mathbf{x} - \epsilon) - v_\theta(\mathbf{x}_t, t, c)\|_2^2] \quad (4)$$

which contrasts with the stochastic differential equations used in Denoising Diffusion Probabilistic Models (DDPM) by employing deterministic optimal transport paths.

Input	Planning	Acting	Reflection	Correction
Generate image with caption: An AI Generated Image <i>a photo of a person and an apple</i> Plan then generate: give dense caption and layout then draw	<p>"dense caption":  <i>"The image shows a person sitting at a table with a shiny red apple in front of him. The background is softly blurred, suggesting a cozy indoor setting, possibly a cafe or restaurant, with warm lighting and a welcoming ambiance. The person is dressed casually, wearing a comfortable blue sweater and glasses, and his short hair frames his face. The scene captures a moment of casual enjoyment, as the apple adds a pop of color to the minimalist arrangement on the table."</i>          "bbox":  <i>[{"an apple.": "0.564,0.703,0.824,0.975"}, {"a person.": "0.199,0.082,0.994,0.99"}]</i></p>			
Generate image with caption: An AI Generated Image <i>a photo of three birds</i> Plan then generate: give dense caption and layout then draw	<p>"dense caption":  <i>"The image shows three small birds perched on a branch. The birds have distinctive plumage patterns, including orange and gray feathers, black beaks, and bright blue wings. They are sitting in a row, facing forward, and appear to be observing their surroundings. The background is blurred, focusing attention on the birds."</i>          "bbox":  <i>[{"three birds.": "0.648,0.359,0.824,0.711"}, {"three birds.": "0.268,0.361,0.447,0.707"}, {"three birds.": "0.451,0.379,0.639,0.709"}]</i></p>			
Generate image with caption: An AI Generated Image <i>a photo of a purple dog above a black dining table</i> Plan then generate: give dense caption and layout then draw	<p>"dense caption":  <i>"The image depicts a modern, minimalist setting with a sleek, black rectangular table as the central focus. The overall atmosphere is clean, highlighted by a cute, fluffy purple dog sitting playfully on the table. The background features a wooden wall with vertical paneling. In front of the table, there are two chairs with a light-colored fabric, suggesting a contemporary design aesthetic."</i>          "bbox":  <i>[{"a purple dog.": "0.293,0.418,0.684,0.74"}, {"a black dining table.": "0.125,0.525,0.996,0.99"}]</i></p>			

Figure 4: Comprehensive examples for each step of Multi-modal Chain of Thought (MCoT).

## 3.2. MINT Architecture Design

### 3.2.1. INPUT REPRESENTATION

Text inputs  $T$  are transformed into an embedding sequence  $\mathbf{x}_{\text{text}} \in \mathbb{R}^{L \times d}$  using Qwen2's tokenizer (Bai et al., 2023), where  $L$  is the sequence length and  $d$  is the embedding dimension. An image  $I \in \mathbb{R}^{H \times W \times 3}$ , with height  $H$  and width  $W$ , is encoded into a latent representation using SD3's Variational Autoencoder (VAE) (Esser et al., 2024b). Following the approach from Transfusion (Zhou et al., 2024b), we compress  $2 \times 2$  patches into a single vector, resulting in image tokens  $\mathbf{x}_{\text{image}} \in \mathbb{R}^{\frac{H}{16} \times \frac{W}{16} \times d}$  after linear projection, where each token corresponds to a  $16 \times 16$  pixel patch of the original image. To accommodate and differentiate the newly introduced image representations, we have expanded the original vocabulary of Qwen2, which consists of 151,936 entities, by incorporating 6 functional special tokens.

### 3.2.2. MIXTURE OF TRANSFORMER EXPERTS

**Experts Design.** We design the mixture of transformer experts (MTXpert) module as the core of the MINT model, which is composed of parallel-arranged experts optimized according to their respective training objectives, thereby alleviating conflicts caused by the coupling of modalities and capabilities (Liang et al., 2024a), and then facilitating the expansion to additional new modalities.

Specifically, MTXpert comprises a Linguistic Expert, a Generative Vision Expert, and a Semantic Vision Expert, all of which have  $L$  layers and fundamentally consistent structures. Linguistic Expert is essentially the same as Qwen2, initialized using the pre-trained Qwen2-0.5B model, to preserve capabilities in language understanding, language generation,

multilingual proficiency, and reasoning. The initialization method for the other two visual experts, as well as the detailed model training strategy, are elaborated in Appendix A. Each expert has independent weights for all non-embedding model parameters, including projection matrices in the attention module, feed-forward networks, and layer normalization, yet sharing the multimodal routing module and global multimodal attention module.

Without loss of generality, we denote  $\mathbf{x} = \mathbf{x}_T \oplus \mathbf{x}_C \oplus \mathbf{x}_N$  as the input, respectively text tokens  $\mathbf{x}_{text}$ , clean image tokens  $\mathbf{x}_{clean}$ , noise  $\mathbf{x}_{noised}$  as  $\mathbf{x}_T, \mathbf{x}_C, \mathbf{x}_N$ , and then describe MTXpert in a configuration with a single layer follows:

$$\begin{aligned}
 \hat{\mathbf{x}}_T, \hat{\mathbf{x}}_C, \hat{\mathbf{x}}_N &= \mathbf{Router}(\mathbf{LN}(\mathbf{x}_T \oplus \mathbf{x}_C \oplus \mathbf{x}_N)) \\
 \hat{\mathbf{x}}_T^q, \hat{\mathbf{x}}_T^k, \hat{\mathbf{x}}_T^v &= \mathbf{W}_T^Q(\hat{\mathbf{x}}_T), \mathbf{W}_T^K(\hat{\mathbf{x}}_T), \mathbf{W}_T^V(\hat{\mathbf{x}}_T) \\
 \hat{\mathbf{x}}_C^q, \hat{\mathbf{x}}_C^k, \hat{\mathbf{x}}_C^v &= \mathbf{W}_C^Q(\hat{\mathbf{x}}_C), \mathbf{W}_C^K(\hat{\mathbf{x}}_C), \mathbf{W}_C^V(\hat{\mathbf{x}}_C) \\
 \hat{\mathbf{x}}_N^q, \hat{\mathbf{x}}_N^k, \hat{\mathbf{x}}_N^v &= \mathbf{W}_N^Q(\hat{\mathbf{x}}_N), \mathbf{W}_N^K(\hat{\mathbf{x}}_N), \mathbf{W}_N^V(\hat{\mathbf{x}}_N) \\
 \mathbf{x}^{\hat{rep}} &= \hat{\mathbf{x}}_T^{\hat{rep}} \oplus \hat{\mathbf{x}}_C^{\hat{rep}} \oplus \hat{\mathbf{x}}_N^{\hat{rep}}, rep \in q, k, v \\
 \hat{\mathbf{x}} &= \mathbf{Attn}(\hat{\mathbf{x}}^q, \hat{\mathbf{x}}^k, \hat{\mathbf{x}}^v) + \mathbf{x}
 \end{aligned} \tag{5}$$

where  $\oplus$  indicates concat operation, *blue*, *red*, *green* respectively for Linguistic Expert, Semantic Visual Expert and Generative Visual Expert modules. And *Attn* module refers to Multimodal Attention which is explained in next section. Then following FFN module can be expressed as:

$$\begin{aligned}
 \hat{\mathbf{x}}_T, \hat{\mathbf{x}}_C, \hat{\mathbf{x}}_N &= \mathbf{Router}(\mathbf{LN}(\mathbf{x}_T \oplus \mathbf{x}_C \oplus \mathbf{x}_N)) \\
 \hat{\mathbf{x}}_T, \hat{\mathbf{x}}_C, \hat{\mathbf{x}}_N &= \mathbf{FFNT}(\hat{\mathbf{x}}_T), \mathbf{FFNC}(\hat{\mathbf{x}}_C), \mathbf{FFNN}(\hat{\mathbf{x}}_N) \\
 \hat{\mathbf{x}} &= \hat{\mathbf{x}}_T \oplus \hat{\mathbf{x}}_C \oplus \hat{\mathbf{x}}_N
 \end{aligned} \tag{6}$$

**Multimodal Attention.** Despite the decoupling of expert parameters, we engage all experts in deep interaction and alignment at each layer through a multimodal attention mechanism. We explain the multimodal attention design from both local and global perspectives. (a) At the local level, we employ different attention patterns for the language and vision modalities. For the language modality, the attention mask adheres to the causal attention pattern. In the case of the vision modality, which includes both clean and noisy images, we use bidirectional attention among all tokens of each individual image since images are physically continuous representations and do not have a natural causal sequence order. (b) At the global level, the global attention mask for all modal data follows the causal attention pattern based on their sequential arrangement, facilitating efficient computation of loss and gradients over an entire sequence in a single forward-backward pass without leaking information from future tokens.

MTXpert, parallel-arranged experts structure, imposes no limit on the potential of newly introduced modality capabilities while seamlessly preserving understanding, generation, and reasoning abilities of the original pre-trained language model. The multimodal attention mechanism facilitates deep modality interaction and alignment among the experts, thereby supporting profound multimodal thinking and reasoning which are vital for MCoT. Consequently, MTXpert demonstrates exceptional potential in addressing complex multimodal tasks and expanding modal capabilities.

### 3.3. Multimodal Chain of Thought for Enhanced Image Generation

For the first time, We introduce the MCoT training paradigm to activate the native MCoT capabilities of unified generative models, facilitating step-by-step multimodal thinking, reasoning, and reflection specifically designed to enhance image generation. Similar to CoT, we define MCoT as a series of multimodal thinking and reasoning intermediate steps: Planning, Acting, Reflection, and Correction, aiming at explicitly unlocking fine-grained multimodal alignment and understanding, thereby improving thinking and reasoning abilities.

MCoT replaces the straightforward T2I generation process with multiple reasoning steps. Specifically, the four steps are grouped into Planning and Acting, as well as Reflection and Correction, based on the two key image generation steps in the foundational process. In Section 3.3.1, we elaborate on the planning and acting processes that address most issues related to intricate image generation with interwoven conditions during the first stage. Meanwhile, the reflection and correction processes focus on resolving region artifacts and alignment discrepancies within the image, as discussed in Section 3.3.2.

#### 3.3.1. PLANNING AND ACTING

Generating intricate images—such as those featuring multiple objects, complex spatial relationships, and various attributes that are all interwoven—requires nuanced, element-wise decoupled alignment and a deep understanding of textual and visual components. However, straightforward T2I generation are inadequate to effectively address these challenges.

To explicitly improve the fine-grained, element-wise decoupled alignment between concepts and attributes in images with their corresponding textual elements, we design the planning and acting steps. Specifically, during the planning step, as illustrated in Figure 4, MINT drafts a more comprehensive and precise image caption without distorting the meaning of the input prompt. In detail, MINT performs both caption planning and layout planning. Caption planning enhances image generation quality through more detailed and comprehensive descriptions, while layout planning generates the spatial layout based on the relationships between concepts, represented by bounding boxes for each object’s position. These two steps foster textual CoT and cross-modal CoT for conceptual and spatial visual awareness, thereby enhancing the model’s inherent capability for joint text-image understanding, multimodal reasoning particularly in detail drafting and spatial reasoning.

Subsequently, in the acting step, MINT generates images informed by the dense draft developed during the planning stage, effectively reducing the confusion often linked to short captions and enhancing the quality of intricate image generation, thereby promoting adherence to interwoven conditions. Ultimately, these two steps further bolster the model’s capacity to fully grasp the semantic connections among the visual concepts and elements, along with their corresponding text, enabling the generated images that are firmly grounded in the logical relationships between them.

#### 3.3.2. REFLECTION AND CORRECTION

Despite employing the aforementioned planning and acting operations to enhance image generation capabilities, the model still struggles to render all parts of an image perfectly in a single generation attempt, following issues such as artifacts, low aesthetic quality, and discrepancies with the corresponding caption. To address these challenges, we propose the reflection step, which enable MINT to self-assess regions of low aesthetic quality, self-reflect artifacts within the generated image, and identify discrepancies between the image and the corresponding caption. Build upon this, the correction step optimizes the image using the insights gained from the reflection step.

Specifically, as illustrated in Figure 3 and 4, during the reflection step, MINT leverages the generated image and

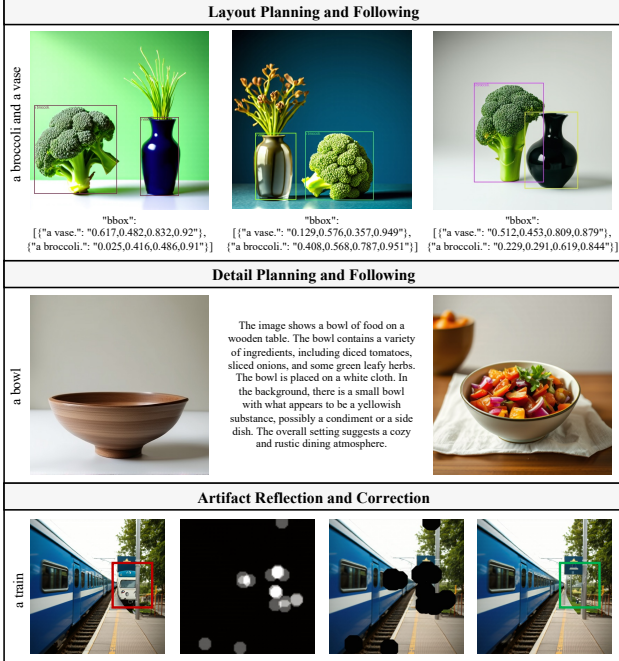


Figure 5: New capabilities integrated into MINT through MCoT. Layout planning enhances spatial reasoning and then adherence to fine-grained positioning instructions, while detail planning improves detail drafting by automatically adding rich details to images, preserving their original meaning and thereby enhancing image quality. Furthermore, the model features self-reflection capabilities that enable it to evaluate and correct image artifacts in a human-like manner, further optimizing image quality.

the input prompt as inputs to identify regions exhibiting artifacts, low aesthetic quality, and misalignments with the input prompt. This process produces an artifact heatmap that quantifies the confidence scores of areas requiring correction, wherein a higher confidence score signifies a more pronounced necessity for adjustments. Furthermore, the reflection process empowers MINT to unlock cross-modal chain-of-thought (CoT) reasoning for both image evaluation and text-image element-wise alignment, and to self-reflect in a human-like manner for leading to more accurate, reliable, and aesthetically pleasing results.

In the correction step, MINT integrates artifact reflection and planning rationales into the generation process, as illustrated in Figure 3, and performs targeted inpainting corrections to refine the artifacts regions that are masked in image based on the artifact heatmap. This process endows MINT with inpainting capability, ultimately effectively addressing issues such as artifacts and aesthetic deficiencies and then producing a higher-quality image that aligns more closely with the intended vision and corresponding caption.

## 4. Experiments

### 4.1. Experimental Details

**Implemental Details.** We employ AdamW (Loshchilov & Hutter, 2017) as the optimizer with parameter setting of  $\beta_1 = 0.9$ ,  $\beta_2 = 0.999$ , and a weight decay of 0.02. The learning rate is configured to a constant value of  $5 \times 10^{-5}$ , incorporating a linear warm-up phase over 10,000 steps. The training utilized DeepSpeed’s ZeRO-2 (Rajbhandari et al., 2020) optimization.

**Evaluation Benchmarks.** We rigorously evaluate the performance of our model using a comprehensive suite of benchmarks tailored for assessing both image generation and image understanding capabilities. (I) Image Generation Evaluation: We employ the MS-COCO dataset (Lin et al., 2014) alongside two key metrics: Fréchet Inception Distance (FID) (Heusel et al., 2017) and CLIP Score (Radford et al., 2021). Additionally, we leverage the GenEval benchmark (Ghosh et al., 2024) to further assessment of enhanced image generation capability, as it offers a holistic framework for assessing generative models across various dimensions. (II) Image Understanding Evaluation: We reference a series of benchmarks that include the MS-COCO with CIDEr score (Vedantam et al., 2015), VQA-v2 (Goyal et al., 2017), MME (Fu et al., 2024), and MMBench (Liu et al., 2024d).

### 4.2. Evaluation for Enhanced Image Generation

The results presented in Table 1 provide a comprehensive evaluation of enhanced image generation capabilities across various models, including image-only unimodal generative models and unified generative models. The upper half of the table highlights unimodal models (image-only), while the lower half features multimodal models capable of generating both images and text.

MINT, our proposed method, achieves an overall score of 0.73, surpassing all other models in its category. For the single-object generation task, MINT scores 0.98, matching the highest scores from unimodal models like SD v2.1 (0.98) and SD 3 (0.98). This performance reflects its ability to accurately generate detailed representations of isolated subjects, likely due to the dense caption planning utilized in the MCoT framework.

In the two-object generation task, MINT scores 0.82, significantly outperforming models such as DALL-E 2 (0.66) and SEED-X (0.58). This demonstrates MINT’s robust capability in composing complex scenes that involve interactions between multiple subjects. Regarding the counting task, MINT achieves a score of 0.66, which is notably superior to other unified generative models and comparable to SD 3, indicating its enhanced ability to accurately manage and represent quantities of generated objects.

Table 1: **Comparison of enhanced image generation quality on GenEval benchmark.** "Uni." refers to unimodal generative models that operate exclusively on images, while "Multi." indicates multimodal generative models that are capable of generating both images and text.

Model	Params	Type	Overall↑	Single Obj.	Two Obj.	Counting	Colors	Position	Attr. Binding
SD v1.5 (Rombach et al., 2022)	1B	Uni.	0.43	0.97	0.38	0.35	0.76	0.04	0.06
SD v2.1 (Rombach et al., 2022)	1.3B	Uni.	0.50	0.98	0.51	0.44	0.85	0.07	0.17
SD-XL (Podell et al., 2024)	3.4B	Uni.	0.55	0.98	0.74	0.39	0.85	0.15	0.23
SD 3 (Esser et al., 2024a)	12.7B	Uni.	0.68	0.98	0.84	0.66	0.74	0.40	0.43
DALL-E 2 (Ramesh et al., 2022)	4.5B	Uni.	0.52	0.94	0.66	0.49	0.77	0.10	0.19
DALL-E 3 (Betker et al., 2023)	—	Uni.	0.67	0.96	0.87	0.47	0.83	0.43	0.45
IF-XL (DeepFloyd, 2023)	10.1B	Uni.	0.61	0.97	0.74	0.66	0.81	0.13	0.35
Chameleon (Team, 2024a)	34B	Multi.	0.39	—	—	—	—	—	—
Transfusion (Zhou et al., 2024a)	7.3B	Multi.	0.63	—	—	—	—	—	—
LWM (Liu et al., 2024c)	7B	Multi.	0.47	0.93	0.41	0.46	0.79	0.09	0.15
SEED-X (Ge et al., 2024a)	17B	Multi.	0.49	0.97	0.58	0.26	0.80	0.19	0.14
Show-o (Xie et al., 2024a)	1.3B	Multi.	0.53	0.95	0.52	0.49	0.82	0.11	0.28
Janus (Wu et al., 2024a)	1.3B	Multi.	0.61	0.97	0.68	0.30	0.84	0.46	0.42
JanusFlow (Ma et al., 2024)	1.3B	Multi.	0.63	0.97	0.59	0.45	0.83	0.53	0.42
<b>MINT (Ours)</b>	1.3B	Multi.	<b>0.73</b>	<b>0.98</b>	<b>0.82</b>	<b>0.66</b>	0.79	<b>0.55</b>	<b>0.56</b>

Table 2: **Performance of foundational image generation capabilities on the MS COCO benchmark.** The asterisk (\*) indicates that the CIDEr results are calculated based on 30K randomly sampled data from the MS-COCO validation set, rather than the standard Karpathy test split set.

Model	Params	FID↓	CLIP Score↑	CIDEr↑
<i>Uni-modal Generative Model</i>				
SD v1.5 (Rombach et al., 2022)	1B	9.93	30.2	—
SD-XL (Podell et al., 2024)	3.4B	—	31.0	—
DALL-E 2 (Ramesh et al., 2022)	4.5B	10.39	31.4	—
DALL-E 3 (Betker et al., 2023)	—	—	32.0	—
IF-XL (DeepFloyd, 2023)	10.1B	6.66	—	—
Emu2-GEN (Sun et al., 2024a)	37B	—	29.7	—
<i>Multi-modal Generative Model</i>				
DREAMLLM (Dong et al., 2024)	7B	—	—	115.4
Chameleon (Team, 2024b)	7B	26.74	24.3	120.2
Transfusion (Zhou et al., 2024b)	7.3B	6.78	25.5	32.0*
SEED-LLaMA (Ge et al., 2023)	8B	—	—	123.6
MetaMorph (Tong et al., 2024)	8B	11.8	—	—
Emu 3 (Wang et al., 2024b)	8B	12.8	31.3	—
LLamaFusion (Shi et al., 2024)	8B	8.61	24.4	38.4*
LLaVAFusion (Shi et al., 2024)	8B	8.28	24.7	—
NExT-GPT (Wu et al., 2024b)	13B	10.07	—	124.9
Show-o (Xie et al., 2024a)	1.3B	9.24	—	—
Janus (Wu et al., 2024a)	1.3B	8.5	—	—
<b>MINT (Ours)</b>	1.3B	7.83	25.2	125.3

In positioning tasks, MINT excels over DALL-E-3 (0.43), showcasing a solid understanding of spatial relationships among objects. Its impressive performance in generating images with multiple objects and diverse spatial arrangements can be attributed to the inherent layout planning capabilities derived from the native MCoT framework. By leveraging its robust multimodal understanding and reasoning abilities, MINT effectively plans and arranges object placements in advance, ensuring consistency in both quantity and positioning.

In terms of color generation, MINT scores 0.79, which is

Table 3: **Comparison results of foundational image understanding performance.**

Model	Params	MME-P↑	MMBench↑	VQA-v2↑
<i>Uni-modal Generative Model</i>				
MobileVLM (Chu et al., 2023)	2.7B	1288.9	59.6	—
LLaVA-Phi (Zhu et al., 2024)	2.7B	1335.1	59.8	71.4
LLaVA (Liu et al., 2024b)	7B	809.6	38.7	—
LLaVA-v1.5 (Liu et al., 2024a)	7B	1510.7	64.3	78.5
Qwen-VL-Chat (Bai et al., 2023)	7B	1487.5	60.6	78.2
IDEFICS-9B (Laurençon et al., 2023)	8B	—	48.2	50.9
Emu3-Chat (Wang et al., 2024b)	8B	—	58.5	75.1
InstructBLIP (Da et al., 2023)	13B	1212.8	—	—
LLaVA-v1.5-Phi-1.5 (Xie et al., 2024a)	1.3B	1128.0	—	75.3
MobileVLM (Chu et al., 2023)	1.4B	1196.2	53.2	—
MobileVLM-V2 (Chu et al., 2024)	1.4B	1302.8	57.7	—
<i>Multi-modal Generative Model</i>				
LWM (Liu et al., 2024c)	7B	—	—	55.8
VILA-U (Wu et al., 2024c)	7B	1401.8	—	79.4
LaVIT (Jin et al., 2024)	7B	—	—	66.0
Chameleon(Team, 2024a)	7B	—	35.7	—
Emu (Sun et al., 2024b)	13B	—	—	52.0
NExT-GPT (Wu et al., 2024b)	13B	—	—	66.7
LLaVAFusion (Shi et al., 2024)	—	—	72.1	—
Gemini-Nano-1 (Team, 2023)	1.8B	—	—	62.7
Show-o (Xie et al., 2024a)	1.3B	948.4	—	59.3
JanusFlow (Ma et al., 2024)	1.3B	1333.1	74.9	79.8
Janus (Wu et al., 2024a)	1.3B	1338.0	69.4	77.3
<b>MINT (Ours)</b>	1.3B	1335.2	70.6	78.3

comparable to the highest-scoring model, SD-XL (0.85), despite having fewer parameters (1.3B vs. 3.4B). This reflects MINT's ability to produce rich and diverse color schemes that enhance the visual quality of generated images.

Finally, in attribute binding tasks, MINT scores 0.56, representing a 24.4% improvement over DALL-E 3 (0.45) and significantly exceeding all other unimodal and unified generative models. This highlights MINT's enhanced capability to manage the complexities of attribute composition, demonstrating superior consistency in text-image alignment, which is crucial for unified generative applications.

In summary, MINT, with its inherent MCoT capabilities, demonstrates outstanding performance across various image

generation tasks, particularly in enhancing the generation of complex images that require nuanced alignment and reasoning between text and visuals.

### 4.3. Foundational Image Generation and Understanding

**Image Generation.** We utilize the MS-COCO dataset to evaluate the foundational image generation capabilities of various generative models. As shown in Table 2, MINT, with a parameter count of 1.3 billion, stands out among its competitors. Notably, MINT achieves a FID score of 7.83, which is significantly lower than many unimodal and multimodal generative models, such as DALL-E 2 (FID of 10.39) and NExT-GPT (FID of 10.07). This suggests that MINT excels in generating higher-quality images. In terms of the CLIP score, MINT scores 25.2, which is comparable to Transfusion’s score of 25.5, despite having considerably fewer parameters (1.3B vs. 7.3B). This indicates that MINT maintains a strong correlation with text.

Moreover, MINT achieved a CIDEr score of 125.3, surpassing all other models in comparison, particularly demonstrating significant advantages in multimodal generative frameworks. This outcome highlights MINT’s capability to generate images that are highly consistent with text descriptions, reinforcing its effectiveness in generative tasks.

**Image Understanding.** As shown in Table 3, we present the results of our experiments on various image understanding benchmarks, comparing MINT against several state-of-the-art models to demonstrate its efficacy in the field of image understanding tasks. MINT achieves an impressive MME-P score of 1335.2, surpassing several unimodal generative models with comparable parameter counts, such as MobileVLM-V2 and Show-o, and closely aligning with leading models despite having only 1.3 billion parameters. This underscores MINT’s effectiveness in tackling complex image understanding challenges. In the MMBench evaluation, MINT scores 70.6, outperforming notable competitors like Janus and LLaVA-v1.5, which highlights its strong capabilities in multimodal scenarios.

Furthermore, MINT attains a VQA-v2 score of 78.3, positioning it among the top performers in visual question answering and directly competing with robust models like LLaVA-v1.5 and Qwen-VL-Chat. Overall, MINT demonstrates exceptional performance across various image understanding benchmarks, establishing itself as a highly competitive model within both unimodal and multimodal generative frameworks.

### 4.4. Ablation Study

In our ablation study, we evaluate the effectiveness of MCoT for enhanced image generation across various configurations, as detailed in Table 4. Since MCoT training is built

Table 4: **Ablation results on GenEval Benchmark for validating the effectiveness of MCoT.**

Task	Generation Style		
	T2I Gen. Twice	MCoT Planning & Acting Only	MCoT Full Process
Single Obj.	0.97	0.97	0.98
Two Obj.	0.80	0.84	0.82
Counting	0.58	0.63	0.66
Colors	0.78	0.81	0.79
Position	0.40	0.50	0.55
Attr. Binding	0.47	0.53	0.56
Overall	0.67	0.71	0.73

upon pretrained MINT model, to ensure a fair comparison, we conduct additional training steps for the baseline using the basic multimodal training paradigm (T2I and I2T) on the same checkpoint, effectively eliminating potential biases arising from increased training iterations. Moreover, as the full MCoT process involves two image generation steps, we maintain fairness by requiring the baseline model to perform T2I generation twice during testing and selecting the best result as the foundational reference for subsequent experiments. The baseline model ultimately yields an overall score of 0.67 on GenEval benchmark.

**Planning and Acting.** Building upon the same pretrained MINT model, we conduct MCoT training and utilize only planning and acting steps for image generation. Notably, in this configuration, image generation is performed only once. As shown in the second column, we observe a significant performance improvement, with the score increasing from 0.67 to 0.71. This underscores the effectiveness of incorporating planning and acting mechanisms in enhancing the model’s capability to generate intricate images. We attribute this improvement to three key factors: (1) a comprehensive understanding of textual and visual components, (2) explicit and nuanced element-wise decoupled alignment, and (3) advanced multimodal reasoning capabilities, particularly in spatial reasoning.

**Reflection and Correction.** Furthermore, with the inclusion of the *Reflection & Correction* mechanism, as shown in the last column, the final performance increases to 0.73. This demonstrates that the reflection and correction steps significantly enhance the quality of the generated results. We attribute this improvement to the model’s self-reflection capability, which enables it to identify artifacts within the image, assess discrepancies between the image and the text prompt, and automatically implement corrective adjustments.

### 4.5. Qualitative Analysis

**MCoT v.s. Straightforward T2I.** As illustrated by the failed results in the first row of Figure 2, several issues

arise: (1) concept confusion in multiple-object generation, (2) spatial confusion in layout instruction generation, (3) attribute confusion in interwoven condition generation, and (4) partial object defects.

Specifically, we attribute concept confusion to the scarcity of uncommon object combinations in nature. Addressing this issue requires the model to possess a comprehensive and precise understanding of object concepts in both the textual and visual domains, which is enhanced by our MCoT framework through explicit fine-grained alignment. Additionally, spatial confusion stems from weak spatial perception and misalignment between fine-grained layout instructions and their corresponding visual outputs. This is mitigated by the layout planning and acting steps in MCoT, which endow MINT with spatial reasoning capabilities.

Moreover, in mixed-attribute image generation tasks, the interleaving of multiple attributes can hinder the model’s ability to accurately follow each detail. MCoT addresses this challenge through nuanced element-wise decoupled alignment and advanced multimodal reasoning. Finally, due to the complexity and abundance of elements in generated images, single-pass generation can result in regional defects. MINT, equipped with reflection and correction mechanisms, demonstrates a clear advantage in this regard, as it significantly improves image quality through automatic assessment and correction at the regional detail level.

## 5. Conclusions

We present **MINT**, an advanced unified generative model that leverages a native multimodal chain of thought (MCoT) to enhance image generation. Our model incorporates a Mixture of Transformer Experts (MTXpert) architecture that effectively balances natural language processing and visual capabilities. By implementing an innovative MCoT training paradigm, MINT achieves nuanced element-wise alignment and promotes advanced multimodal reasoning and self-reflection. As a result, MINT demonstrates superior performance in text-to-image (T2I) and image-to-text (I2T) tasks across multiple benchmarks, addressing the challenges of generating intricate images.

## References

Bachmann, R., Kar, O. F., Mizrahi, D., Garjani, A., Gao, M., Griffiths, D., Hu, J., Dehghan, A., and Zamir, A. 4m-21: An any-to-any vision model for tens of tasks and modalities. *arXiv preprint arXiv:2406.09406*, 2024.

Bai, J., Bai, S., Yang, S., Wang, S., Tan, S., Wang, P., Lin, J., Zhou, C., and Zhou, J. Qwen-VL: A frontier large vision-language model with versatile abilities. *arXiv preprint arXiv:2308.12966*, 2023.

Betker, J., Goh, G., Jing, L., Brooks, T., Wang, J., Li, L., Ouyang, L., Zhuang, J., Lee, J., Guo, Y., et al. Improving image generation with better captions. *Computer Science*, 2023.

Brooks, T., Holynski, A., and Efros, A. A. Instructpix2pix: Learning to follow image editing instructions. In *CVPR*, pp. 18392–18402, 2023.

Chen, Z., Wu, J., Wang, W., Su, W., Chen, G., Xing, S., Zhong, M., Zhang, Q., Zhu, X., Lu, L., et al. Internvl: Scaling up vision foundation models and aligning for generic visual-linguistic tasks. In *CVPR*, pp. 24185–24198, 2024.

Chu, X., Qiao, L., Lin, X., Xu, S., Yang, Y., Hu, Y., Wei, F., Zhang, X., Zhang, B., Wei, X., et al. MobileVLM: A fast, reproducible and strong vision language assistant for mobile devices. *arXiv preprint arXiv:2312.16886*, 2023.

Chu, X., Qiao, L., Zhang, X., Xu, S., Wei, F., Yang, Y., Sun, X., Hu, Y., Lin, X., Zhang, B., et al. MobileVLM V2: Faster and stronger baseline for vision language model. *arXiv preprint arXiv:2402.03766*, 2024.

Dai, W., Li, J., Li, D., Tiong, A. M. H., Zhao, J., Wang, W., Li, B., Fung, P., and Hoi, S. InstructBLIP: Towards general-purpose vision-language models with instruction tuning. In *Proc. Annu. Conf. Neural Inf. Process. Systems*, 2023.

DeepFloyd. DeepFloyd IF, 2023. URL <https://huggingface.co/DeepFloyd/IF-I-XL-v1.0>.

Ding, M., Yang, Z., Hong, W., Zheng, W., Zhou, C., Yin, D., Lin, J., Zou, X., Shao, Z., Yang, H., et al. Cogview: Mastering text-to-image generation via transformers. In *NeurIPS*, 2021.

Dong, R., Han, C., Peng, Y., Qi, Z., Ge, Z., Yang, J., Zhao, L., Sun, J., Zhou, H., Wei, H., et al. DreamLLM: Synergistic multimodal comprehension and creation. In *Proc. Int'l Conf. Learning Representations*, 2024.

Esser, P., Kulal, S., Blattmann, A., Entezari, R., Müller, J., Saini, H., Levi, Y., Lorenz, D., Sauer, A., Boesel, F., et al. Scaling rectified flow transformers for high-resolution image synthesis. In *Proc. Int'l Conf. Machine Learning*, 2024a.

Esser, P., Kulal, S., Blattmann, A., Entezari, R., Müller, J., Saini, H., Levi, Y., Lorenz, D., Sauer, A., Boesel, F., et al. Scaling rectified flow transformers for high-resolution image synthesis. In *Forty-first International Conference on Machine Learning*, 2024b.

- Fu, C., Chen, P., Shen, Y., Qin, Y., Zhang, M., Lin, X., Yang, J., Zheng, X., Li, K., Sun, X., Wu, Y., and Ji, R. MME: A comprehensive evaluation benchmark for multimodal large language models. *arXiv preprint arXiv:2306.13394*, 2024.
- Gan, Y., Park, S., Schubert, A., Philippakis, A., and Alaa, A. M. Instructcv: Instruction-tuned text-to-image diffusion models as vision generalists. *arXiv preprint arXiv:2310.00390*, 2023.
- Gao, J., Liu, Y., Sun, Y., Tang, Y., Zeng, Y., Chen, K., and Zhao, C. Styleshot: A snapshot on any style. *arXiv preprint arXiv:2407.01414*, 2024.
- Ge, Y., Zhao, S., Zeng, Z., Ge, Y., Li, C., Wang, X., and Shan, Y. Making llama see and draw with seed tokenizer. *arXiv preprint arXiv:2310.01218*, 2023.
- Ge, Y., Zhao, S., Zhu, J., Ge, Y., Yi, K., Song, L., Li, C., Ding, X., and Shan, Y. SEED-X: Multimodal models with unified multi-granularity comprehension and generation. *arXiv preprint arXiv:2404.14396*, 2024a.
- Ge, Y., Zhao, S., Zhu, J., Ge, Y., Yi, K., Song, L., Li, C., Ding, X., and Shan, Y. Seed-x: Multimodal models with unified multi-granularity comprehension and generation. *arXiv preprint arXiv:2404.14396*, 2024b.
- Geng, Z., Yang, B., Hang, T., Li, C., Gu, S., Zhang, T., Bao, J., Zhang, Z., Li, H., Hu, H., et al. Instructdiffusion: A generalist modeling interface for vision tasks. In *CVPR*, pp. 12709–12720, 2024.
- Geva, M., Khashabi, D., Segal, E., Khot, T., Roth, D., and Berant, J. Did aristotle use a laptop? a question answering benchmark with implicit reasoning strategies. *Transactions of the Association for Computational Linguistics*, 9: 346–361, 2021.
- Ghosh, D., Hajishirzi, H., and Schmidt, L. GenEval: An object-focused framework for evaluating text-to-image alignment. In *Proc. Annu. Conf. Neural Inf. Process. Systems*, 2024.
- Goyal, Y., Khot, T., Summers-Stay, D., Batra, D., and Parikh, D. Making the v in VQA matter: Elevating the role of image understanding in visual question answering. In *Proc. IEEE Int'l Conf. Computer Vision and Pattern Recognition*, 2017.
- He, W., Fu, S., Liu, M., Wang, X., Xiao, W., Shu, F., Wang, Y., Zhang, L., Yu, Z., Li, H., et al. Mars: Mixture of auto-regressive models for fine-grained text-to-image synthesis. *arXiv preprint arXiv:2407.07614*, 2024.
- Heusel, M., Ramsauer, H., Unterthiner, T., Nessler, B., and Hochreiter, S. GANs trained by a two time-scale update rule converge to a local nash equilibrium. In *Proc. Annu. Conf. Neural Inf. Process. Systems*, 2017.
- Ho, J., Chan, W., Saharia, C., Whang, J., Gao, R., Gritsenko, A., Kingma, D. P., Poole, B., Norouzi, M., Fleet, D. J., et al. Imagen video: High definition video generation with diffusion models. *arXiv preprint arXiv:2210.02303*, 2022.
- Jin, Y., Xu, K., Chen, L., Liao, C., Tan, J., Huang, Q., Bin, C., Song, C., ZHANG, D., Ou, W., et al. Unified language-vision pretraining in llm with dynamic discrete visual tokenization. In *Proc. Int'l Conf. Learning Representations*, 2024.
- Ju, X., Liu, X., Wang, X., Bian, Y., Shan, Y., and Xu, Q. Brushnet: A plug-and-play image inpainting model with decomposed dual-branch diffusion. In *European Conference on Computer Vision*, pp. 150–168. Springer, 2024.
- Kondratyuk, D., Yu, L., Gu, X., Lezama, J., Huang, J., Schindler, G., Hornung, R., Birodkar, V., Yan, J., Chiu, M.-C., et al. Videopoet: A large language model for zero-shot video generation. *arXiv preprint arXiv:2312.14125*, 2023.
- Laurençon, H., van Strien, D., Bekman, S., Tronchon, L., Saulnier, L., Wang, T., Karamcheti, S., Singh, A., Pisitilli, G., Jernite, Y., et al. Introducing IDEFICS: An open reproduction of state-of-the-art visual language model, 2023, 2023. URL <https://huggingface.co/blog/idefics>.
- Liang, W., Yu, L., Luo, L., Iyer, S., Dong, N., Zhou, C., Ghosh, G., Lewis, M., Yih, W.-t., Zettlemoyer, L., et al. Mixture-of-transformers: A sparse and scalable architecture for multi-modal foundation models. *arXiv preprint arXiv:2411.04996*, 2024a.
- Liang, Y., He, J., Li, G., Li, P., Klimovskiy, A., Carolan, N., Sun, J., Pont-Tuset, J., Young, S., Yang, F., et al. Rich human feedback for text-to-image generation. In *Proceedings of the IEEE/CVF Conference on Computer Vision and Pattern Recognition*, pp. 19401–19411, 2024b.
- Lin, T.-Y., Maire, M., Belongie, S., Hays, J., Perona, P., Ramanan, D., Dollár, P., and Zitnick, C. L. Microsoft coco: Common objects in context. In *Proc. European Conf. Computer Vision*, 2014.
- Liu, H., Li, C., Wu, Q., and Lee, Y. J. Visual instruction tuning. In *NeurIPS*, 2023.
- Liu, H., Li, C., Li, Y., and Lee, Y. J. Improved baselines with visual instruction tuning. In *Proc. IEEE Int'l Conf. Computer Vision and Pattern Recognition*, 2024a.

- Liu, H., Li, C., Wu, Q., and Lee, Y. J. Visual instruction tuning. In *Proc. Annu. Conf. Neural Inf. Process. Systems*, 2024b.
- Liu, H., Yan, W., Zaharia, M., and Abbeel, P. World model on million-length video and language with ringattention. *arXiv preprint arXiv:2402.08268*, 2024c.
- Liu, Y., Duan, H., Zhang, Y., Li, B., Zhang, S., Zhao, W., Yuan, Y., Wang, J., He, C., Liu, Z., et al. MMBench: Is your multi-modal model an all-around player? In *Proc. European Conf. Computer Vision*, 2024d.
- Loshchilov, I. and Hutter, F. Decoupled weight decay regularization. *arXiv preprint arXiv:1711.05101*, 2017.
- Lu, J., Clark, C., Lee, S., Zhang, Z., Khosla, S., Marten, R., Hoiem, D., and Kembhavi, A. Unified-io 2: Scaling autoregressive multimodal models with vision language audio and action. In *CVPR*, pp. 26439–26455, 2024.
- Ma, Y., Liu, X., Chen, X., Liu, W., Wu, C., Wu, Z., Pan, Z., Xie, Z., Zhang, H., Zhao, L., et al. Janusflow: Harmonizing autoregression and rectified flow for unified multimodal understanding and generation. *arXiv preprint arXiv:2411.07975*, 2024.
- Mou, C., Wang, X., Xie, L., Wu, Y., Zhang, J., Qi, Z., and Shan, Y. T2i-adapter: Learning adapters to dig out more controllable ability for text-to-image diffusion models. In *AAAI*, volume 38, pp. 4296–4304, 2024.
- OpenAI. GPT-4 technical report. *arXiv:2303.08774*, 2023.
- Podell, D., English, Z., Lacey, K., Blattmann, A., Dockhorn, T., Müller, J., Penna, J., and Rombach, R. SDXL: Improving latent diffusion models for high-resolution image synthesis. In *Proc. Int'l Conf. Learning Representations*, 2024.
- Radford, A., Kim, J. W., Hallacy, C., Ramesh, A., Goh, G., Agarwal, S., Sastry, G., Askell, A., Mishkin, P., Clark, J., et al. Learning transferable visual models from natural language supervision. In *Proc. Int'l Conf. Machine Learning*, 2021.
- Rajbhandari, S., Rasley, J., Ruwase, O., and He, Y. Zero: Memory optimizations toward training trillion parameter models, 2020.
- Ramesh, A., Dhariwal, P., Nichol, A., Chu, C., and Chen, M. Hierarchical text-conditional image generation with CLIP latents. *arXiv preprint arXiv:2204.06125*, 2022.
- Ren, T., Liu, S., Zeng, A., Lin, J., Li, K., Cao, H., Chen, J., Huang, X., Chen, Y., Yan, F., et al. Grounded sam: Assembling open-world models for diverse visual tasks. *arXiv preprint arXiv:2401.14159*, 2024.
- Rombach, R., Blattmann, A., Lorenz, D., Esser, P., and Ommer, B. High-resolution image synthesis with latent diffusion models. In *Proc. IEEE Int'l Conf. Computer Vision and Pattern Recognition*, 2022.
- Sheynin, S., Polyak, A., Singer, U., Kirstain, Y., Zohar, A., Ashual, O., Parikh, D., and Taigman, Y. Emu edit: Precise image editing via recognition and generation tasks. In *CVPR*, pp. 8871–8879, 2024.
- Shi, W., Han, X., Zhou, C., Liang, W., Lin, X. V., Zettlemoyer, L., and Yu, L. Llamafusion: Adapting pretrained language models for multimodal generation. *arXiv preprint arXiv:2412.15188*, 2024.
- Sun, Q., Cui, Y., Zhang, X., Zhang, F., Yu, Q., Wang, Y., Rao, Y., Liu, J., Huang, T., and Wang, X. Generative multimodal models are in-context learners. In *CVPR*, pp. 14398–14409, 2024a.
- Sun, Q., Yu, Q., Cui, Y., Zhang, F., Zhang, X., Wang, Y., Gao, H., Liu, J., Huang, T., and Wang, X. Generative pre-training in multimodality. In *Proc. Int'l Conf. Learning Representations*, 2024b.
- Team, C. Chameleon: Mixed-modal early-fusion foundation models. *arXiv preprint arXiv:2405.09818*, 2024a.
- Team, C. Chameleon: Mixed-modal early-fusion foundation models. *arXiv preprint arXiv:2405.09818*, 2024b.
- Team, G. Gemini: a family of highly capable multimodal models. *arXiv preprint arXiv:2312.11805*, 2023.
- Tong, S., Fan, D., Zhu, J., Xiong, Y., Chen, X., Sinha, K., Rabat, M., LeCun, Y., Xie, S., and Liu, Z. Metamorph: Multimodal understanding and generation via instruction tuning. *arXiv preprint arXiv:2412.14164*, 2024.
- Vedantam, R., Lawrence Zitnick, C., and Parikh, D. Cider: Consensus-based image description evaluation. In *Proceedings of the IEEE conference on computer vision and pattern recognition*, pp. 4566–4575, 2015.
- Wang, P., Bai, S., Tan, S., Wang, S., Fan, Z., Bai, J., Chen, K., Liu, X., Wang, J., Ge, W., et al. Qwen2-vl: Enhancing vision-language model's perception of the world at any resolution. *arXiv preprint arXiv:2409.12191*, 2024a.
- Wang, W., Lv, Q., Yu, W., Hong, W., Qi, J., Wang, Y., Ji, J., Yang, Z., Zhao, L., Song, X., et al. Cogylm: Visual expert for pretrained language models. *arXiv preprint arXiv:2311.03079*, 2023.
- Wang, X., Zhang, X., Luo, Z., Sun, Q., Cui, Y., Wang, J., Zhang, F., Wang, Y., Li, Z., Yu, Q., et al. Emu3: Next-token prediction is all you need. *arXiv preprint arXiv:2409.18869*, 2024b.

- Wei, J., Wang, X., Schuurmans, D., Bosma, M., Xia, F., Chi, E., Le, Q. V., Zhou, D., et al. Chain-of-thought prompting elicits reasoning in large language models. *Advances in neural information processing systems*, 35:24824–24837, 2022a.
- Wei, J., Wang, X., Schuurmans, D., Bosma, M., Xia, F., Chi, E., Le, Q. V., Zhou, D., et al. Chain-of-thought prompting elicits reasoning in large language models. *Advances in neural information processing systems*, 35:24824–24837, 2022b.
- Wu, C., Chen, X., Wu, Z., Ma, Y., Liu, X., Pan, Z., Liu, W., Xie, Z., Yu, X., Ruan, C., et al. Janus: Decoupling visual encoding for unified multimodal understanding and generation. *arXiv preprint arXiv:2410.13848*, 2024a.
- Wu, S., Fei, H., Qu, L., Ji, W., and Chua, T.-S. NExT-GPT: Any-to-any multimodal LLM. In *Proc. Int'l Conf. Machine Learning*, 2024b.
- Wu, Y., Zhang, Z., Chen, J., Tang, H., Li, D., Fang, Y., Zhu, L., Xie, E., Yin, H., Yi, L., et al. VILA-U: A unified foundation model integrating visual understanding and generation. *arXiv preprint arXiv:2409.04429*, 2024c.
- Xiao, S., Wang, Y., Zhou, J., Yuan, H., Xing, X., Yan, R., Wang, S., Huang, T., and Liu, Z. Omnigen: Unified image generation. *arXiv preprint arXiv:2409.11340*, 2024.
- Xie, J., Mao, W., Bai, Z., Zhang, D. J., Wang, W., Lin, K. Q., Gu, Y., Chen, Z., Yang, Z., and Shou, M. Z. Show-o: One single transformer to unify multimodal understanding and generation. *arXiv preprint arXiv:2408.12528*, 2024a.
- Xie, J., Mao, W., Bai, Z., Zhang, D. J., Wang, W., Lin, K. Q., Gu, Y., Chen, Z., Yang, Z., and Shou, M. Z. Show-o: One single transformer to unify multimodal understanding and generation. *arXiv preprint arXiv:2408.12528*, 2024b.
- Xu, G., Jin, P., Hao, L., Song, Y., Sun, L., and Yuan, L. Llava-o1: Let vision language models reason step-by-step. *arXiv preprint arXiv:2411.10440*, 2024.
- Zhang, L., Rao, A., and Agrawala, M. Adding conditional control to text-to-image diffusion models. In *ICCV*, pp. 3836–3847, 2023.
- Zhou, C., Yu, L., Babu, A., Tirumala, K., Yasunaga, M., Shamis, L., Kahn, J., Ma, X., Zettlemoyer, L., and Levy, O. Transfusion: Predict the next token and diffuse images with one multi-modal model. *arXiv preprint arXiv:2408.11039*, 2024a.
- Zhou, C., Yu, L., Babu, A., Tirumala, K., Yasunaga, M., Shamis, L., Kahn, J., Ma, X., Zettlemoyer, L., and Levy, O. Transfusion: Predict the next token and diffuse images with one multi-modal model. *arXiv preprint arXiv:2408.11039*, 2024b.
- Zhu, Y., Zhu, M., Liu, N., Ou, Z., Mou, X., and Tang, J. LLaVA-Phi: Efficient multi-modal assistant with small language model. *arXiv preprint arXiv:2401.02330*, 2024.

## A. Train Strategy

### A.1. Pre-training for T2I and I2T

We adopt a two-stage training approach to systematically integrate the text-to-image (T2I) and image-to-text (I2T) capabilities of the MINT model.

**Stage I:** In this initial stage, we focus on optimizing the T2I functionality of MINT by training the model specifically for the T2I task. Both the Linguistic Expert and the Generative Visual Expert are trained, with their parameters initialized from the Qwne2-0.5B model. The image resolution for this phase is configured to  $256 \times 256$  pixels.

**Stage II:** During this stage, MINT undergoes mixed training, encompassing both T2I and I2T tasks at a training task ratio of 8:1. The I2T tasks include image captioning and Visual Question Answering (VQA). In this phase, all experts are trainable, and the newly introduced Semantic Visual Expert is initialized using parameters from the Generative Visual Expert established in Stage I. The resolution of images at this stage is increased to  $512 \times 512$ .

### A.2. Multimodal Chain of Thought Training

After the pretraining phase, MINT possesses capabilities for image generation and image understanding, enabled by the any2any task paradigm supported within MNIT. We decompose the MCoT training into a multi-task format that separately supports planning and acting, reflection, and correction. Specifically, for the planning and acting task, the model takes a short caption as input and produces a dense caption along with the coordinates of the objects planned in the image. For the reflection task, the model receives a generated image and short caption as input and predicts the corresponding artifact/implausibility heatmap(Liang et al., 2024b). For the correction task, we achieve this through training on inpainting tasks. It is noteworthy that all of these tasks are trained simultaneously within the same unified model.

## B. Dataset Construction

### B.1. Pre-training Data

In **Stage I** of the pre-training process, we utilized approximately 250 million image-text pairs to train the text-to-image (T2I) task. In **Stage II**, due to the increased resource demands associated with higher image resolutions, we improved the quality of images and captions through filtering and recaptioning techniques. Specifically, we employed an aesthetic model to curate high-quality images, and utilized the Qwen-VL(Wang et al., 2024a) and CogVLM(Wang et al., 2023) models to generate refined, high-quality captions for these images. Ultimately, we collected and constructed a dataset comprising approximately 80 million samples for image generation task and 10 million samples for image understanding task.

### B.2. MCoT Data

To construct the dataset for the planning and acting stage, we utilized Qwen-VL (Wang et al., 2024a) to generate dense captions. Subsequently, we extracted all object description phrases from the dense captions and employed Grounded SAM (Ren et al., 2024) to generate the corresponding grounding boxes. For the reflection task, we leveraged the RichHF-18K dataset (Liang et al., 2024b) and the additional 5,000 images generated by MNIT, which were manually annotated to identify the bounding boxes of incorrectly generated objects, along with their corresponding prompt contents. For the inpainting correction task (for correction), we followed the methodology outlined in BrushNet (Ju et al., 2024) to generate random masks and segmentation masks.